

# Polychromatic nonlinear surface modes generated by supercontinuum light

Andrey A. Sukhorukov<sup>1</sup>, Dragomir N. Neshev<sup>1</sup>,  
Alexander Dreischuh<sup>1,2</sup>, Robert Fischer<sup>1</sup>, Sangwoo Ha<sup>1</sup>,  
Wieslaw Krolikowski<sup>1</sup>, Jeremy Bolger<sup>3</sup>, Arnan Mitchell<sup>4</sup>,  
Benjamin J. Eggleton<sup>3</sup>, and Yuri S. Kivshar<sup>1</sup>

<sup>1</sup>*Nonlinear Physics Centre and Laser Physics Centre, Centre for Ultra-high bandwidth Devices for Optical Systems (CUDOS), Research School of Physical Sciences and Engineering, Australian National University, Canberra ACT 0200, Australia*

<sup>2</sup>*Department of Quantum Electronics, Faculty of Physics, Sofia University, Bulgaria*

<sup>3</sup>*School of Physics and Centre for Ultra-high bandwidth Devices for Optical Systems (CUDOS), University of Sydney, Sydney NSW 2006, Australia*

<sup>4</sup>*School of Electrical and Computer Systems Engineering, RMIT University, Melbourne Vic 3001, Australia*

[ans124@rsphysse.anu.edu.au](mailto:ans124@rsphysse.anu.edu.au)

**Abstract:** We study propagation of polychromatic light near the edge of a nonlinear waveguide array. We describe simultaneous spatial and spectral beam reshaping associated with power and wavelength-dependent tunneling between the waveguides. We present experimental verifications of the effects predicted theoretically including the first observation of supercontinuum nonlinear surface modes.

© 2006 Optical Society of America

**OCIS codes:** (190.4420) Nonlinear optics, transverse effects in; (190.5940) Self-action effects

---

## References and links

1. K. G. Makris, S. Suntsov, D. N. Christodoulides, G. I. Stegeman, and A. Hache, "Discrete surface solitons," *Opt. Lett.* **30**, 2466–2468 (2005).
2. S. Suntsov, K. G. Makris, D. N. Christodoulides, G. I. Stegeman, A. Hache, R. Morandotti, H. Yang, G. Salamo, and M. Sorel, "Observation of discrete surface solitons," *Phys. Rev. Lett.* **96**, 063901–4 (2006).
3. Y. V. Kartashov, V. A. Vysloukh, and L. Torner, "Surface gap solitons," *Phys. Rev. Lett.* **96**, 073901–4 (2006).
4. G. A. Siviloglou, K. G. Makris, R. Iwanow, R. Schiek, D. N. Christodoulides, G. I. Stegeman, Y. Min, and W. Sohler, "Observation of discrete quadratic surface solitons," *Opt. Express* **14**, 5508–5516 (2006), <http://www.opticsinfobase.org/abstract.cfm?URI=oe-14-12-5508>.
5. C. R. Rosberg, D. N. Neshev, W. Krolikowski, A. Mitchell, R. A. Vicencio, M. I. Molina, and Yu. S. Kivshar, "Observation of surface gap solitons in semi-infinite waveguide arrays," *Phys. Rev. Lett.* **97**, 083901–4 (2006).
6. E. Smirnov, M. Stepic, C. E. Ruter, D. Kip, and V. Shandarov, "Observation of staggered surface solitary waves in one-dimensional waveguide arrays," *Opt. Lett.* **31**, 2338–2340 (2006).
7. K. Motzek, A. A. Sukhorukov, and Yu. S. Kivshar, "Polychromatic interface solitons in nonlinear photonic lattices," *Opt. Lett.* **31**, 3125–3127 (2006).
8. M. Mitchell and M. Segev, "Self-trapping of incoherent white light," *Nature* **387**, 880–883 (1997).
9. H. Buljan, T. Schwartz, M. Segev, M. Soljacic, and D. N. Christodoulides, "Polychromatic partially spatially incoherent solitons in a noninstantaneous Kerr nonlinear medium," *J. Opt. Soc. Am. B* **21**, 397–404 (2004).
10. R. Pezer, H. Buljan, G. Bartal, M. Segev, and J. W. Fleischer, "Incoherent white-light solitons in nonlinear periodic lattices," *Phys. Rev. E* **73**, 056608–9 (2006).
11. J. K. Ranka, R. S. Windeler, and A. J. Stentz, "Visible continuum generation in air-silica microstructure optical fibers with anomalous dispersion at 800 nm," *Opt. Lett.* **25**, 25–27 (2000).
12. P. St. J. Russell, "Photonic crystal fibers," *Science* **299**, 358–362 (2003).
13. M. Matuszewski, C. R. Rosberg, D. N. Neshev, A. A. Sukhorukov, A. Mitchell, M. Trippenbach, M. W. Austin, W. Krolikowski, and Yu. S. Kivshar, "Crossover from self-defocusing to discrete trapping in nonlinear waveguide arrays," *Opt. Express* **14**, 254–259 (2006), <http://www.opticsinfobase.org/abstract.cfm?URI=oe-14-1-254>.

14. P. Yeh, A. Yariv, and C. S. Hong, "Electromagnetic propagation in periodic stratified media .1. General theory," *J. Opt. Soc. Am.* **67**, 423–438 (1977).
15. P. Yeh, A. Yariv, and A. Y. Cho, "Optical surface waves in periodic layered media," *Appl. Phys. Lett.* **32**, 104–105 (1978).
16. K. Motzek, A. A. Sukhorukov, Yu. S. Kivshar, and F. Kaiser, "Polychromatic multigap solitons in nonlinear photonic lattices," In *Nonlinear Guided Waves and Their Applications*, Postconference ed. OSA p. WD25 (Optical Society of America, Washington DC, 2005).
17. K. Motzek, A. A. Sukhorukov, and Yu. S. Kivshar, "Self-trapping of polychromatic light in nonlinear periodic photonic structures," *Opt. Express* **14**, 9873–9878 (2006), <http://www.opticsinfobase.org/abstract.cfm?URI=oe-14-21-9873>.

## 1. Introduction

Self-action of the monochromatic light or parametric interaction with the second-harmonic field near the edge of a nonlinear periodic structure can lead to the formation of localized nonlinear surface modes or surface solitons [1, 2, 3, 4, 5, 6]. The physics of surface solitons is based on creation of self-induced surface defects through an effective nonlinear change of optical refractive index. More general polychromatic nonlinear surface modes can be excited by light beams with a supercontinuum frequency spectrum [7]. It was predicted that collective nonlinear interaction of multiple spectral components at the interface of two different photonic lattices may lead to selective filtering for red- or blue-shifted frequencies that is controlled by the input power. In this work, we describe theoretically and demonstrate experimentally flexible power-controlled reshaping of polychromatic light beams near the edge of the nonlinear waveguide array where the linear refractive index of the surface waveguide is slightly modified. We show that the beam propagation depends strongly on the input position with respect to the surface defect, and we reveal novel possibilities for the power-dependent and wavelength-selective manipulation of light components from the visible to infrared, utilizing the broadband response of the photorefractive nonlinearity. We also present the first experimental observation of polychromatic surface modes generated by supercontinuum radiation.

## 2. Nonlinear reshaping of polychromatic light at surfaces: theoretical analysis

We study propagation of polychromatic light in an array of coupled optical waveguides created in a LiNbO<sub>3</sub> substrate, where the formation of monochromatic surface solitons due to photorefractive nonlinear response was recently demonstrated in experiment [5, 6]. Photorefractive nonlinearity is based on a relatively slow charge accumulation, and therefore the induced refractive index can be defined by the time-averaged light intensity of different spectral components [8, 9, 10]. We consider an optical source with the high degree of spatial coherence, such as *supercontinuum light generated in photonic-crystal fibers* [11, 12]. Then, the evolution of such polychromatic beams can be described by a set of normalized nonlinear equations for the spatial beam envelopes  $A_m(x, z)$  of different frequency components at vacuum wavelengths  $\lambda_m$ ,

$$i \frac{\partial A_m}{\partial z} + \frac{\lambda_m z_s}{4\pi n_0 x_s^2} \frac{\partial^2 A_m}{\partial x^2} + \frac{2\pi z_s}{\lambda_m} \left\{ v(x) + \frac{\gamma}{M} \sum_{j=1}^M \sigma(\lambda_j) |A_j|^2 \right\} A_m = 0, \quad (1)$$

where  $x$  and  $z$  are the dimensionless transverse and longitudinal coordinates normalized to  $x_s = 10\mu\text{m}$  and  $z_s = 1\text{mm}$ , respectively,  $n_0 = 2.35$  is the average refractive index,  $v(x)$  is the effective refractive index modulation,  $\gamma$  is the nonlinear coefficient, and  $\sigma(\lambda)$  defines the relative photosensitivity of the medium at various wavelengths. We approximate the photosensitivity dependence in LiNbO<sub>3</sub> waveguides for  $\lambda > 400\text{nm}$  as  $\sigma(\lambda) = \exp[-\log(2)(\lambda - \lambda_b)^2 / \lambda_w^2]$  with  $\lambda_b = 400\text{nm}$  and  $\lambda_w = 150\text{nm}$ , and choose the number of frequency components  $M = 50$  to model accurately the beams with supercontinuum spectrum.

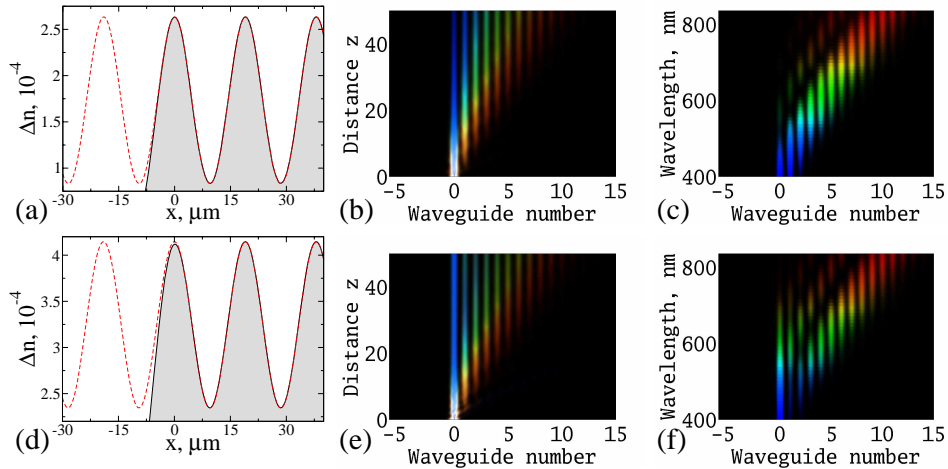


Fig. 1. (a,d) Refractive index profiles in waveguide arrays with (a) weaker (for  $w = 7\mu\text{m}$ ) and (d) stronger (for  $w = 8.5\mu\text{m}$ ) surface defects. Dashed line shows, for comparison, the refractive index in an infinite periodic structure. Corresponding (b,e) dynamics inside the arrays and (c,f) output spectra are shown for the input beam coupled to the surface waveguide. The input spectrum is constant for  $400\text{nm} < \lambda < 830\text{nm}$ .

The refractive index profile of the waveguides created by Ti-indiffusion on  $\text{LiNbO}_3$  substrate can be approximately described [13] as  $v(x) = \xi \sum_{n=0}^N \exp[-(x - nd)^2/w^2]$ , where  $N$  is the total number of waveguides,  $d$  is the period, and  $w$  depends on the width of Ti strips in the fabrication process. The deposited layers of Ti broaden due to diffusion process, creating an overlap that leads to an additional increase of the refractive index in the neighboring waveguides. Since the surface waveguide lacks a neighbor on one side, its refractive index contrast is slightly *lower* than that for other waveguides in the array, and this results in the appearance of a *surface defect*. The refractive index mismatch is increased for stronger overlap of the indiffused regions, i.e. for larger values of  $w$  for the same refractive index contrast in the lattice by an appropriate choice of  $\xi$ , as illustrated in Figs. 1(a,d).

The surface defect plays the role of an optical waveguide when the refractive index change exceeds a certain threshold, such that the mode eigenvalue can be shifted outside the photonic band [14, 15]. Since the bandgap structure of a photonic lattice depends strongly on frequency, the critical change of the refractive index becomes also wavelength-dependent. This effect can be explained using the coupled-mode equations for describing spatial evolution of the amplitudes  $\Psi_n$  of the modes of individual waveguides,  $id\Psi_0/dz + \delta(\lambda)\Psi_0 + C(\lambda)\Psi_1 = 0$ ,  $id\Psi_n/dz + C(\lambda)(\Psi_{n-1} + \Psi_{n+1}) = 0$ , where  $n > 0$  is the waveguide number,  $\delta(\lambda)$  characterizes the strength of a surface defect, and  $C(\lambda)$  is inversely proportional to the coupling length between the neighboring waveguides. These equations admit a solution in the form of a localized surface mode only when  $|\delta(\lambda)| > C(\lambda)$ . Since the coupling coefficient increases and the effective defect strength decreases for longer wavelengths, only the modes with  $\lambda < \lambda_{\text{th}}$  can be localized at the surface, where the cut-off wavelength is defined from the equation  $|\delta(\lambda_{\text{th}})| = C(\lambda_{\text{th}})$ .

We perform numerical simulations of the beam propagation in waveguide arrays with weaker [see Fig. 1(a)] and stronger [see Fig. 1(d)] surface defects. When the beam is coupled to the surface waveguide, all wavelength components escape from the surface in the case of a weak defect, as shown in Figs. 1(b,c). However, a stronger defect can trap blue spectral components whereas the longer wavelength components still escape from the surface due to larger coupling; this is in a perfect agreement with the coupled-mode theory results [see Figs. 1(e,f)].

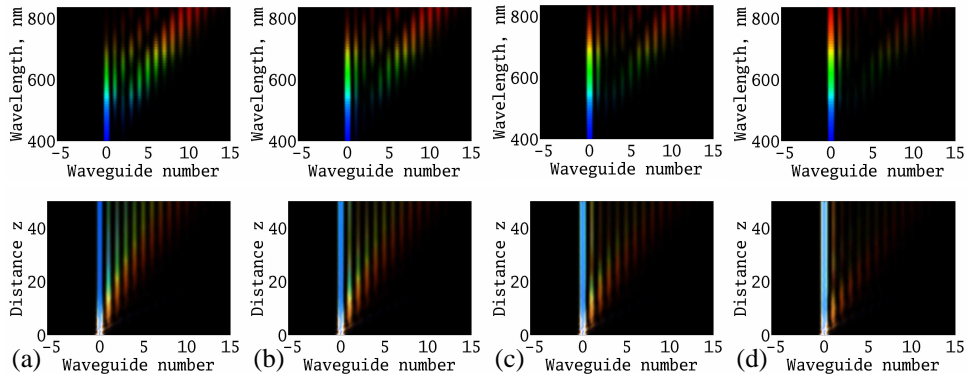


Fig. 2. (a-d) Nonlinear dynamics in the waveguide array (bottom) and corresponding output spectra (top) for increasing powers of the input beam coupled to the surface waveguide. Maximum changes of the nonlinear refractive index at the input ( $z = 0$ ) are  $|\Delta n_{\text{nonl}}| \times 10^5 \simeq 0.3, 0.9, 1.6, 2.8$ . Other parameters correspond to Fig. 1(d).

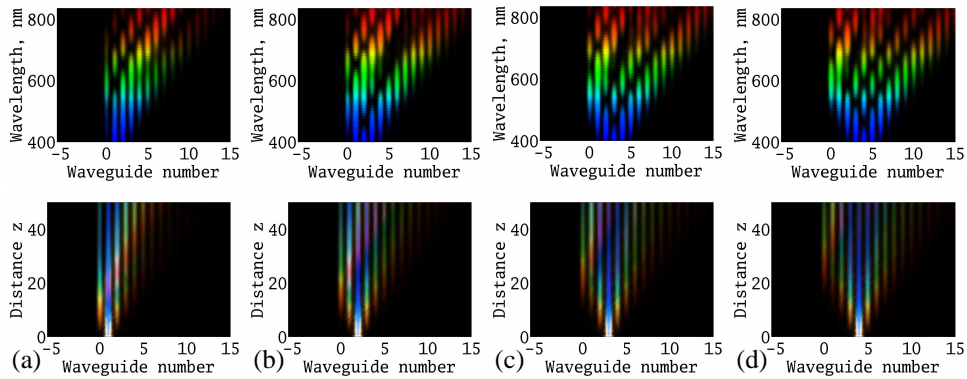


Fig. 3. (a-d) Linear dynamics inside the array (bottom) and corresponding output spectra (top) for different input beam positions. Parameters correspond to Fig. 1(a).

When the beam is coupled to the surface waveguide and the light intensity increases, the refractive index becomes lower through the *defocusing* photovoltaic nonlinearity. This effect can be treated as an effective increase of the defect strength  $|\delta|$ , resulting in progressive trapping at the surface of longer wavelength components when the input power grows. Such continuous tuning of the output beam shape and spectrum is illustrated in Fig. 2.

Very different dynamics is observed when light is coupled to other waveguides away from the surface defect. In the linear regime, the tunneling of short-wavelength components with  $\lambda < \lambda_{\text{th}}$  to the first waveguide is suppressed almost completely. On the other hand, light at longer wavelengths can penetrate in the first waveguide, see Fig. 3.

We analyze in detail the nonlinear dynamics of the beam coupled to the second waveguide ( $n = 1$ ) of the array. As the light intensity grows, the refractive index at the location of the input beam keeps decreasing, approaching gradually the refractive index of the surface waveguide. When the mismatch between the two waveguides is reduced, shorter wavelength components start tunneling to the first waveguide, see Fig. 4(b). As this happens, nonlinearity acts to increase the mismatch, and light switches permanently to the first waveguide, as shown in Fig. 4(c).

For even higher input powers, the refractive index of the second waveguide decreases to

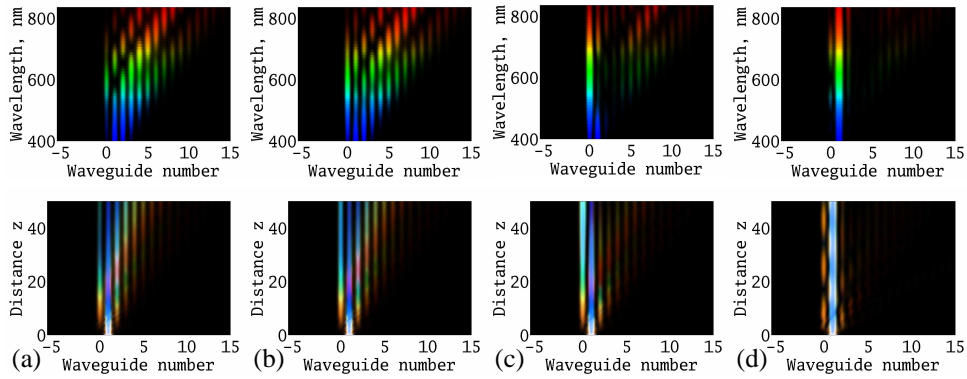


Fig. 4. (a) Linear and (b-d) nonlinear dynamics inside the array (bottom) and output spectra (top) for increasing powers of the input beam coupled to the second ( $n = 1$ ) waveguide. Maximum nonlinear changes of refractive index at the input ( $z = 0$ ) are  $|\Delta n_{\text{nonl}}| \times 10^5 \simeq 0, 1.6, 2.8, 6.2$ . Other parameters correspond to Fig. 1(a).

the values below the index of the neighboring waveguides, such that light remains trapped at the input location, as shown in Fig. 4(d). Similar self-trapping regime at high powers is also observed for other input beam positions away from the surface, approaching the regime for the formation of polychromatic soliton formation in infinite photonic lattices [16, 17].

### 3. Experimental observation of supercontinuum nonlinear surface modes

We design an array of closely spaced optical waveguides produced by Titanium indiffusion into a monocrystal lithium niobate wafer. The waveguide array has a period of  $19\mu\text{m}$  and effective refractive index contrast  $1.8 \times 10^{-4}$  at wavelength 585nm. In the fabrication process,  $100\text{\AA}$  of Ti was deposited on the X-cut  $\text{LiNbO}_3$  using electron beam evaporation. The Ti layer was then photolithographically patterned and etched in a buffered hydrofluoric acid solution. The diffusion was conducted at  $1050^\circ\text{C}$  for 3 hours in a wet oxygen environment.

In our experiments we used a femtosecond laser (Mira, Coherent) emitting  $\sim 140$  fs pulses at a central wavelength of 800 nm. The fs-laser beam was tightly focused by a microscope objective ( $\times 40$ ) onto the input facet of a 2 m long highly nonlinear photonic crystal fiber (NL-2.0-740) with engineered zero dispersion at 740 nm. The generated supercontinuum spectra [11] spanned over the range of 450 – 850nm. After the fiber end, the supercontinuum radiation is collimated, spectrally analyzed, and its power is controlled by variable attenuator. The light was then tightly focused as an extraordinary beam into a single guide of the  $\text{LiNbO}_3$  waveguide array. The output of the array was then imaged by a microscope objective ( $\times 5$ ) onto a color CCD camera (Philips).

The polychromatic input in a single waveguide near the interface of the waveguide array allowed us to observe wavelength-resolved discrete diffraction [Fig. 5(top row)]. For this purpose, the light at the output of the waveguide array was dispersed by a prism (glass SF-11) before imaging onto the camera. Aligning this equilateral prism for minimum deviation at 532 nm and using the prism dispersive characteristic (calculated by the third-order Sellmeier formula and prism-to-CCD distance) we determined the wavelength scaling in the plane of the detector. Then we traced the intensity distribution at the output in the linear propagation regime (low power) for input beam positioned from the first waveguide inwards the sample. We find that the diffracted light is strongly reflected by the surface [Fig. 5(top row)] and the output spectral energy-density distributions are asymmetric. These observations agree very well with the theo-

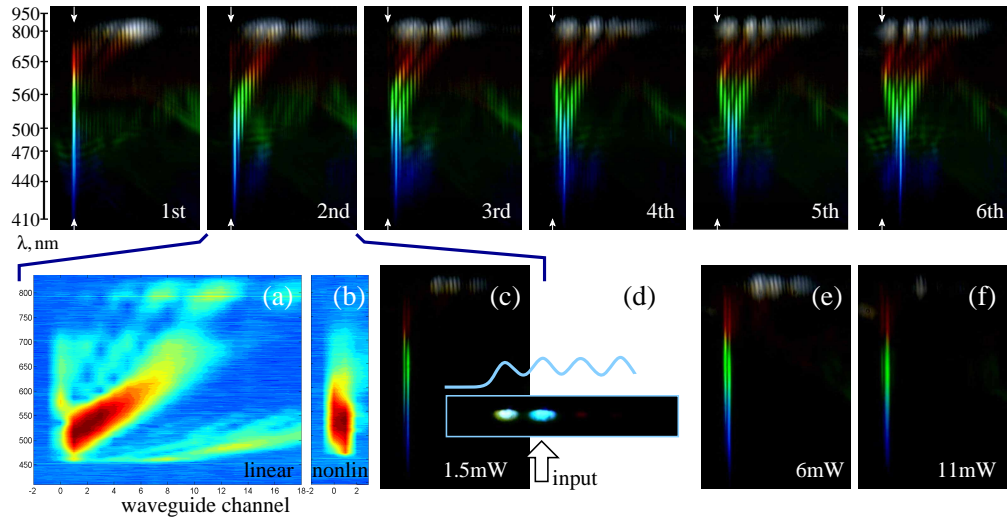


Fig. 5. Experimental demonstration of interaction of a supercontinuum polychromatic light with a surface. *Top row*: Output spectrally resolved spatial distribution at low powers of  $32 \mu\text{W}$  (linear propagation) for input beam positioned at the first ( $n = 0$ ), second ( $n = 1$ ), ... and the sixth ( $n = 5$ ) waveguide respectively. *Bottom row*: Excitation at the second waveguide. (a) Linear spectral distribution measured by a spectrometer. The position “zero” ( $n = 0$ ) indicates the edge waveguide of the array. The intensity is represented in logarithmic scale for better visualization. (b,c) Corresponding nonlinear localization (b) measured by a spectrometer and (c) spectrally resolved spatial distribution for input power of  $1.25 \text{ mW}$ . (d) Output intensity distribution and the corresponding refractive index profile of the waveguide array. (e,f) Spectrally resolved spatial distribution at higher input powers of  $6$  and  $11 \text{ mW}$ , respectively.

retical predictions [Fig. 3(top row)]. The colors at the images represent the natural colors of the supercontinuum, except for the near-infrared part of the spectrum, which are detected as white by the camera. For the case of initial excitation at the second waveguide of the array the results were also verified by using a spectrometer [Fig. 5(a)].

Due to the strong photovoltaic effect in the  $\text{LiNbO}_3$  sample it exhibits a nonlinear response of defocusing type. As the input power into the second waveguide is increased, we observe enhanced coupling of red, green, and blue components to the surface waveguide [Figs. 5(b-e)] and the formation of polychromatic surface modes. At even higher powers the second waveguide is fully detuned from the neighboring ones and we observed light trapping entirely in the second waveguide [Figs. 5(f)] and the influence of the surface is thus strongly reduced. This behavior follows precisely the tendencies predicted in the theoretical analysis [Figs. 4(top row)].

#### 4. Conclusions

We have described theoretically and demonstrated experimentally tunable spatial reshaping of supercontinuum light in an array of nonlinear optical waveguides. We have shown that all-optical wavelength-selective switching between the output waveguides can be realized by introducing surface defects, and we have presented the first experimental observation of polychromatic nonlinear surface modes generated by a source with supercontinuum spectrum.

This work was partially supported by the Australian Research Council and NSF-Bulgaria grant WUF-02/05.